Using Synthetic Data Trained Convolutional Neural Network For Predicting Sub-Resolution Thin Layers From Seismic Data

Dongfang Qu[1,3]*, Klaus Mosegaard[2], Runhai Feng[2], Lars Nielsen[1]

1. Department of Geosciences and Natural Resource Management, University of Copenhagen, Øster Voldgade 10, 1350 Copenhagen, Denmark
2. Niels Bohr institute, University of Copenhagen, 2200 Copenhagen, Denmark
3. Ramboll Danmark A/S, Hannemanns Allé 53, 2300 Copenhagen, Denmark

*Corresponding author (qudongfang2012@gmail.com)

Interpretation®

USING SYNTHETIC DATA TRAINED CONVOLUTIONAL NEURAL NETWORK FOR PREDICTING SUB-RESOLUTION THIN LAYERS FROM SEISMIC DATA

Journal:	*Interpretation*
Manuscript ID	INT-2022-0059
Manuscript Type:	Technical Paper (if no special section applies)
Date Submitted by the Author:	19-May-2022
Complete List of Authors:	Qu, Dongfang; University of Copenhagen; Rambøll A/S, Mosegaard, Klaus; University of Copenhagen: the Niels Bohr Institute, Department of Physics Feng, Runhai ; University of Copenhagen, Niels Bohr Institute Nielsen, Lars; University of Copenhagen, Department of Geosciences and Natural Resource Management
Keywords:	seismic, artificial intelligence, geostatistics, layered, reservoir characterization
Subject Areas:	Structural, stratigraphic, and sedimentologic interpretation, Interpretation concepts, algorithms, methods, and tools, Application examples (applying a relatively new technique or concept), Near-surface, ground penetrating radar, environmental, and engineering applications, Outcrop and subsurface modeling

USING SYNTHETIC DATA TRAINED CONVOLUTIONAL NEURAL NETWORK FOR PREDICTING SUB-RESOLUTION THIN LAYERS FROM SEISMIC DATA

Dongfang Qu[1,3]*(qudongfang2012@gmail.com), Klaus Mosegaard[2] (mosegaard@nbi.ku.dk), Runhai Feng[2] (runhai.feng@gmail.com), Lars Nielsen[1] (ln@ign.ku.dk)

1. Department of Geosciences and Natural Resource Management, University of Copenhagen, Øster Voldgade 10, 1350 Copenhagen, Denmark
2. Niels Bohr institute, University of Copenhagen, 2200 Copenhagen, Denmark
3. Ramboll Danmark A/S, Hannemanns Allé 53, 2300 Copenhagen, Denmark

*Corresponding author

Running head:

SYNTHETIC DATA-TRAINED DEEP LEARNING FOR SEISMIC INTERPRETATION

Original paper date of submission: 19-05-2022

ABSTRACT

Numerous studies have demonstrated the capability of supervised deep learning techniques for predicting geological features of interest from seismic sections, including features that are difficult to identify using traditional interpretation methods. However, successful application of these techniques in practice has been limited by the difficulty of obtaining large training dataset where seismic data and corresponding ground truth labels are well defined. Manually creating large amounts of labels requires a heavy workload, and the uncertainty of the interpretation and labeling process decreases the model's ability for making accurate predictions. Using the chalk-flint sequence scenario onshore Denmark as an example, we present a workflow of generating large quantities of synthetic training data with high-quality labels, and we investigate the capability of a synthetic data-trained convolutional neural network for predicting sub-resolution thin layers from seismic sections. We generate the synthetic examples using stochastic geological modeling and seismic forward modeling, and we test the performance of the trained neural network on new synthetic seismic data where more complex bedding architectures are considered, as well as on real seismic data.

INTRODUCTION

With the increasing availability of computing powers, supervised deep learning techniques, particularly the end-to-end convolutional neural network (e.g. U-net), have been increasingly used for predicting geological features of interest from seismic data (Li et al., 2019; Wu et al., 2019; Feng et al., 2021). They have shown advantages in not only higher efficiency but also capability for predicting features that are normally difficult to identify as compared to traditional interpretation methods (Dramsch, 2020). A critical factor for achieving success using this approach is the availability of large amounts of training data where seismic data and corresponding ground truth labels are well defined (Merrifield et al., 2022). This is difficult as data in geoscience is often expensive, sparse, uncertain and biased, some are not even machine-readable (Dramsch, 2020). Creating large amounts of labels requires firstly interpreting the geological features of interest from seismic data, and then manual labelling, which may not be feasible in practice. Moreover, the uncertainties related to such an interpretation and labeling process can decrease the model's ability for making accurate predictions.

One way of generating large quantities of training data with high quality labels is to create synthetic data (Merrifield et al., 2022). Several deep learning projects used synthetically generated seismic data including computer-generated labels for predicting geological features from seismic data sections and produced promising results (e.g. Wu et al., 2019; Merrifield et al., 2022). These existing studies are mainly focused on large-scale features that can be easily identified by the human eye, such as large-scale faults, salt domes, and layers with thicknesses larger than the seismic resolutions. Prediction of thin layers that are below the resolution of seismic data has not been studied. In this paper, we show the capability of synthetic data-trained deep neural network for predicting sub-resolution thin layers from seismic data.

SEISMIC INTERPRETATION CHALLENGES

Mapping the distribution of individual layers of specific lithology or soil type from seismic data is demanded in many geoscience applications, including characterization of near-surface materials at planned construction site, characterization of hydrocarbon and groundwater reservoirs, etc. Yet it is a challenging task as the layers of interest can be too thin to be resolved by the seismic data. Seismic interpretation provides only formation boundaries, not boundaries between sub-resolution layers. Seismic inversion could potentially resolve rock physical properties from which the layer boundaries can be interpreted, but the inversion resolution is limited by e.g. the intrinsic tuning effects, incomplete knowledge of the seismic wavelet and noise in the data (Phan, 2021). Geostatistical seismic inversion makes use of statistical information and could potentially provide a higher inversion resolution, but relies on a geostatistical simulation algorithm generating multiple realistic geological realizations, which becomes difficult when the geometry and spatial arrangement of the layers are too complex to be simulated in an efficient way (Wang et al., 2022).

For example, the chalk and flint layers widely distributed in onshore SE Denmark have contrasting physical and geotechnical properties. Mapping their spatial distribution is needed for e.g. characterization of construction sites and groundwater resource planning, but is also challenging as the abundant and important flint layers are so thin (ca. 20 – 30 cm) that reflected signals from closely spaced layer boundaries interfere with each other and generate misleading composite signals (Qu et al., 2022). Bedding architectures are furthermore variable due to a dynamic depositional environment in which the sediment was formed; horizontal bedding, wavy bedding, onlap, downlap, and pinch-out can coexist in the same sequence and only hand-drawing can reproduce the bedding architectures in full detail (Anderskouv et al., 2007, Qu et al., 2022).

Thus, some questions that are interesting to be investigated are as follows: Is it possible to predict the correct number of thin layers from seismic sections where the reflected signals are highly interfering with each other? Can a neural network trained on synthetic examples with simple and regular layering architectures manage to predict more complex and variable layering architectures? Can a neural network trained on synthetic seismic data make predictions on real seismic data?

In this study, we use the chalk-flint sequence scenario in onshore Denmark as an example, to develop and present a workflow of generating large quantities of relevant and diverse synthetic training data. We investigate the feasibility of a convolutional neural network trained on synthetic data for mapping thin layers with variable geometries from real seismic data. We generate the synthetic examples using stochastic geological modelling and seismic forward modelling, and we then test the performance of the trained neural network on both new synthetic seismic data and real seismic data.

SYNTHETIC TRAINING DATASET

One way to create relevant synthetic examples is to make the most of available information, e.g. previous geological studies about the formation of interest, lithology types revealed by borehole data, outcropping sections of the same formations or other formations deposited in similar environments. In this study, prior knowledge of the geometry and physical properties of the layers in the chalk-flint sequence in onshore Denmark has been taken into consideration for creating the synthetic examples (e.g. Surlyk et al., 2006; Anderskouv et al., 2007; Nielsen et al., 2011; Kammann et al., 2019; Yuan et al., 2021).

Geological models

After obtaining an understanding of the lithology types occurring in the formation of interest and possible thickness and spatial distributions from prior knowledge, we develop a modeling method that can honor the known information. It is important that large amounts of geological models can be generated in an automated, efficient manner without heavy manual work, otherwise the advantage of the synthetic data-trained deep learning approach would be reduced. Our strategy is to make relevant geological models based on known geological information, but ignore some complex bedding architecture features. We will then test the generalization ability of the deep learning model to investigate if it can predict the complex bedding phenomena not included the training examples.

The sequence of interest in this study consists of interbedded chalk and flint layers, in which the thickness of chalk layers varies laterally, while the thickness of flint layers is assumed constant. We generate various interbedded chalk-flint sections using a published carbonate mound modelling strategy that has been published (Janson and Madriz, 2012). The thickness of each chalk layer bounded between two flint layers is modelled using a variogram-based stochastic geostatistical modelling method, i.e., sequential Gaussian simulation (SGS). A flint layer with constant thickness is added on top of each chalk layer. The chalk layer thickness and variogram range of the thickness variation in the lateral direction are chosen randomly with some constraints, which are based on prior knowledge of the geometry of the well-known chalk strata (e.g. Surlyk et al., 2006; Anderskouv et al., 2007). In the case when little information is available about the input parameters, a wide constraining range can be applied for each input parameter to capture different possibilities resulting from the uncertainty.

500 geological sections with different numbers of layers and varying geometries are generated, constrained by a mean chalk layer thickness between 1 and 10 meters and a variogram

range of the thickness variation between 20 and 500 meters. Each section has 256 × 2560 pixels, with each pixel representing 0.1 m in space and 0.07 ms in time (Figure 1). Each flint layer has a constant thickness of three pixels. The chosen resolution is decided by considering the thin thickness of the high-velocity flint layers and the numbers of flint layers to be included in the sections. We would like to have enough pixels to represent the thin and wavy flint layers, but also would like to have the possibility of including more flint layers in the sections such that the interference effect contributed by different numbers of interfaces can be captured.

Two sections of interbedded strata with different numbers of layers and different layer geometries are shown in Figures 1a and b. It needs to be noted that some complex phenomena observed from outcropping sections, such as wedge-shaped onlap, are not included in the synthetic examples. It would be a huge advantage of this approach if the model trained on examples with simple bedding phenomena can predict complex bedding phenomena. We will train a model using this dataset including only simple bedding phenomena and apply it on cases exhibiting complex phenomena not present in the training dataset. Thus the generalization ability of the deep learning model on unseen data with unseen geological features can be tested.

Seismic synthetics

The geological sections are transformed to acoustic impedance sections by assigning realistic P-wave velocity and bulk density values for flint layers and chalk layers, such as 5500 m/s and 2800 kg/m^3 for flint, and 2300 m/s and 2700 kg/m^3 for chalk (Qu et al., 2022). Reflectivity sections are then computed. The seismic images are generated by performing a 2D convolution of the reflectivity matrix and a 2D Ricker wavelet matrix, and returning the central part of the convolution that has the same size as the reflectivity matrix (Figure 1c, d). A 10% white Gaussian noise is added to each seismic image.

Considering the fact that any practical migration will result in a somewhat smoothed response laterally, we use a 2D wavelet with a 'hyperbolic' shape and decreasing amplitude away from the center to simulate an imperfectly migrated response from a point scatterer. The horizontal width and bending of the wavelet take account of the remaining horizontal smearing after data migration, and are adjustable. A wider wavelet produces more horizontal smearing; a more bended wavelet generates synthetics mimicking under-migrated or over-migrated seismic data. In this paper, these parameters are adjusted based on one of our test examples, such that the synthetics generated using this method can be similar to the seismic image used as a test. The dominant frequency of the Ricker wavelet used in this paper is 150 Hz (Figure 2), consistent with the dominant frequency of our seismic data on which the trained neural network is to be applied.

These 500 pairs of geological sections and corresponding seismic images are then split into 5000 pairs of smaller patches, each has a resolution of 256 × 256 pixels (Figure 3). The amplitude of each big seismic image is scaled to a range between -1 and 1 prior to splitting.

NETWORK TRAINING

Network architecture

For each pixel in the seismic image, we would like to know the category it belongs to (flint layer or not), which is a binary segmentation problem. We use a U-net architecture to perform this segmentation task. U-net was originally developed for biomedical image segmentation (Ronneberger et al., 2015), and it has later on been successfully used for seismic interpretation (Li et al., 2019; Wu et al., 2019). It has an important advantage in requiring less training images and yielding more precise segmentations (Ronneberger et al., 2015).

The U-net that we use for thin layer segmentation consists of a contracting path and a symmetric expanding path that enables precise localization (Figure 4). The left contracting path consists of four convolution groups and each group is followed by a 2 × 2 max pooling to halve the image size. Each convolution group involves two 3 × 3 convolutions, each followed by a ReLU activation (Nair and Hinton 2010) and a batch normalization (Ioffe and Szegedy 2015). In each convolution operation, a feature detector, also known as a kernel or a filter, moves across the layer's input matrix and generates a feature map; the value of each pixel in the feature map is a dot product of the filter with the area of the input matrix around that pixel. A set of learnable filters are applied in each convolution layer, and multiple feature maps are generated. In the contracting path, the image size decreases as the number of channels increases, and the image size reaches a minimum at the bottom. In the right expanding path, every step consists of an operation that doubles the image size and halves the number of feature channels, a concatenation with the corresponding feature image from the contracting path, and two convolutions, each followed by a ReLU activation and a batch normalization. Finally, the output size is restored to that of the original image, which is 256 × 256 in this case. At the end of the network, a 1 × 1 convolution followed by a Sigmoid function (equation 1) outputs the probability of each pixel belonging to category 1 (i.e. the flint layer).

$$S(\mathrm{x}) = \frac{1}{1 + e^{-x}} \tag{1}$$

Loss function

Commonly used loss functions such as binary cross-entropy require a more or less balanced distribution of zeros and non-zeros (Wu et al., 2019; van Beers et al., 2019), which is not the case here, as the geological scenarios are dominated by the chalk background.

In this paper, we use a loss function based on the Jaccard Similarity Coefficient, also known as intersection-over-union (IoU). IoU measures the similarity between the predicted region and the ground-truth region for an object present in the image and is often used as a measure of success. It is defined as the size of the intersection divided by the size of the union of two sets (Rahman and Wang, 2016), and takes into account of the class imbalance issue. The loss function used in this paper is defined in terms of an approximation of the IoU, which becomes differentiable (van Beers et al., 2019). The definition of the metric and loss function used to train the network are written as follows:

$$\text{Metric} = \frac{T * P + 1}{T + P - T * P + 1} \tag{2}$$

$$\text{Loss} = -\frac{T * P + 1}{T + P - T * P + 1} \tag{3}$$

Where T is the True image composed of 1s and 0s, P is the predicted image composed of probability values between 0 and 1, T*P is the element-wise multiplication of T and P.

Training

We use 4250 pairs of the geological and seismic patches as training data and the rest 750 pairs as validation data. The Adam method is used to optimize the network parameters (Kingma and Ba, 2014). The batch size is 32. Number of epochs to train the network is set to 70, but with an early stopping option – training will be stopped if the monitored metric has no improvement after 5 epochs. The learning rate will be reduced with a factor of 0.1 when the metric has stopped improving after 3 epochs, with a minimum learning rate of 0.00001.

Figure 5 shows that the training and validation loss decrease with the increase of epochs, and the loss on the validation set stops decreasing after 45 epochs. We run the proposed network model using NVIDIA Quadro P5000 GPU, and the training takes 20 minutes.

TEST AND RESULTS

We test the performance of the trained neural network on two synthetic examples and one real example. As the neural network is trained on image patches with size of 256 × 256, the seismic images to apply it on are divided into patches of size 256 × 256, on which the predictions are made. The predicted geological image patches are reconstructed to form complete images afterwards.

The prediction outputs probability of each pixel belonging to the category of flint. The probability section is then converted to category sections by using a threshold value of 0.5, i.e. pixels with probability values higher than 0.5 are classified as flint. The prediction results are visually compared to either ground truth labels (if available) or outcropping geological sections nearby the seismic data, and they are evaluated in terms of predicted numbers of flint layers, geometries, and continuity.

Test on synthetic example similar to the training data

We first test the performance of the trained neural network on a synthetic example generated by the same modeling algorithm used for generating the training dataset, but not used in the training and validation process (Figure 6). The ground truth geological scenario is an interbedded sequence consisting of 10 flint layers and 11 chalk layers, all below the seismic resolution (Figure 6b). The strata pattern is similar to that of the training examples; all layers are continuous. The synthetic seismic image shows three to four discontinuous reflections, due to interference of reflected signals from closely spaced layer boundaries (Figure 6a; Qu et al., 2022). These sub-resolution layers are difficult to interpret from the seismic image.

Figure 6c shows the result predicted by the trained neural network. The number of layers, the thickness of each layer, and the gently wavy geometry are well predicted. Continuity artifacts

can be observed at some places (e.g. the red circles in Figure 6c), this is because the flint layers are so thin (only three pixels thick) that any tiny inaccuracy can cause discontinuity. Increasing the resolution of the image might improve the continuity of the predicted layers.

Test on synthetic example different from the training data

It is not surprising that the trained convolutional neural network works well in the first test as the test data are drawn from the same statistics as the ones used for the training data – all have simple strata patterns. The real strata patterns of the onshore chalk succession in SE Denmark are more complex; some units can contain onlap and downlap phenomena, which are not included in the training dataset. Would the convolutional neural network trained on examples with simple bedding architectures be able to extrapolate and predict more complex bedding architectures?

In the second test, we apply the trained model on a seismic section whose ground truth label contains new bedding features such as onlap, downlap and pinch-out (Figure 7b). Interference of reflected signals results in fault-like discontinuities in the reflections, which can lead to misinterpretation (Qu et al., 2022). This seismic image is computed using full-wavefield modelling based on finite difference approach, different from the convolution method used in the generation of the training data, thus can contain different seismic features introduced by smearing effect, multiples, converted waves, as well as further processing such as migration. However, we have tried to reduce the difference caused by different seismic modelling processes. We computed synthetics for the geological model shown in Figure 7b using the convolution method using 2D Ricker wavelets with different parameters, found the 2D Ricker wavelet that can generate a seismic image similar to the one shown in Figure 7a, and used this wavelet to generate the synthetics of the training dataset.

Figure 7c shows the result predicted by the trained neural network. The prediction is successful in terms of the quantity of the individual layers, the thickness and geometry of the layers, and even the complex bedding architectures. In fact, the new features such as onlap and downlap are predicted. Continuity artifacts exist, particularly at places where two flint layers are too close to each other.

Test on real seismic data

The acquisition and processing of seismic data can introduce some complex features that are not present in the synthetic training examples. We now test the trained convolutional neural network with real seismic data - a seismic profile acquired from the upper Maastrichtian–Danian chalk succession at the Stevns peninsula in Denmark (Kammann et al., 2019).

The seismic profile is close to a coastal cliff and a quarry with exposed chalk sections. We apply the trained neural network on the top section of the seismic profile (Figure 8a), so we can assess the quality of the prediction result by comparing to the exposed sections. The succession of interest comprises 20–30m of chalk of latest Cretaceous (Maastrichtian) age and 10–20m of bryozoan limestone of Early Paleocene (Danian) age. The upper Maastrichtian part contains 10–12 flint layers with variable spacing distance (Surlyk et al., 2013), and exhibits gently wavy to almost horizontal bedding. The Danian part contains around 8–10 flint layers with variable spacing distance (Surlyk et al., 2013), and displays mound structures which are typically 50-100 m long (Surlyk et al., 2006; Figure 8b). This seismic data displays complex reflection patterns with undulations and terminations (Figure 8a). It shows weak reflectivity in the top section, and strong reflection at around 20–30 ms, which is consistent with the boundary between the Maastrichtian and Danian formations. This strong reflection can be traced throughout the section, except at an

interruption at distance of 200 meters, which is most likely caused by a low fold. Please refer to Kammann et al. (2019) for details of the acquisition and processing of the data.

Figure 8c shows the result predicted by the trained neural network. The run-time of this prediction process is in the order of seconds. Around 20 flint layers are predicted for this succession, 8–10 wavy flint layers in the Danian formation in the upper succession and 10–12 gently wavy to horizontal flint layers in the Maastrichtian formation in the lower succession. These are consistent with what observed from the outcropping sections. The observed mound structures with typical length of 50–100 m are also predicted. Thus, the trained neural network is able to predict the quantity of flint layers and their geometries, even on real seismic data, which is much noisier than the synthetic training data. Similar with the first two tests, continuity artifacts mostly likely exist. Note that the 2D wavelet (Figure 2) used to generate the synthetic seismic of the training examples has not been particularly adjusted to produce smearing and other effects similar to that of the real seismic, and it is expected that a tailored wavelet can improve the performance of the trained deep learning model.

CONCLUSION

We have illustrated how to generate synthetic training data for supervised deep learning and investigated the capability of deep learning trained on synthetic data for predicting sub-resolution thin layers from seismic data, exemplified by an interbedded chalk-flint sequence scenario in onshore Denmark.

The result is promising as the network is able to predict the approximately correct numbers of thin layers and their geometries from real seismic data, despite the presence of effects such as interference and smearing, which challenge the interpretation of sub-resolution thin layers. The network can also generalize and predict more complex bedding structures not seen before.

Continuity artifacts exist in the predicted results, this is because the flint layers are so thin that even tiny inaccuracy in predicted position can lead to discontinuity; increasing the number of pixels representing the thin layers should be able to improve the continuity. More work can be conducted in the future for improved prediction, e.g., adjusting the wavelet used for computing the synthetics or improving the processing of the real seismic data to minimize their difference, testing different neural network architectures, hyper-parameters and loss functions. Data augmentation may also help to improve the network performance.

The synthetic training dataset is generated via stochastic geological modelling and seismic forward modelling. The presented stochastic geological modeling method allows for the generation of a large number of synthetic examples and incorporation of known geological knowledge which help to generate relevant geological models. The synthetic seismic images are generated by performing a convolution operation between the 2D reflectivity models converted from the geological models and a 2D wavelet. The 2D wavelet can be adjusted to produce seismic features (e.g. smearing effects) similar to those existed in the real seismic data.

We have generated 5000 synthetic seismic images with a dominant frequency of 150 Hz and 5000 ground truth labels, each has 256 × 256 pixels and trained a U-net model, which can be applied to predict the thin flint layers from seismic data acquired from the chalk succession onshore Denmark. We expect that the network model trained by this dataset can also be applied on seismic data acquired from other two-lithofacies geological scenarios with different dominant frequencies, by scaling the time and space interval that each pixel represents. The training dataset is available at https://github.com/GeoDQ/Interbedding_Dataset. We encourage interested readers to train deep learning models using this dataset and explore its applicability on seismic data collected from different geological scenarios, such as interbedded sandstone and shale.

ACKNOWLEDGEMENT

The research leading to these results has received funding from the Danish Hydrocarbon Research and Technology Centre under the AWF-1 program. Janina Kammann is acknowledged for providing the seismic data published in Kammann et al (2019).

REFERENCES

Anderskouv, K., T. Damholt, and F. Surlyk, 2007, Late Maastrichtian chalk mounds, Stevns Klint, Denmark—combined physical and biogenic structures: Sedimentary Geology, **200**, 57-72.

Dramsch, J.S., 2020, 70 years of machine learning in geoscience in review: Advances in geophysics, **61**, 1-55.

Feng, R., D. Grana, and N. Balling, 2021, Uncertainty quantification in fault detection using convolutional neural networks: Geophysics, **86**, 41-48.

Ioffe, S., and C. Szegedy, 2015, Batch normalization: Accelerating deep network training by reducing internal covariate shift, *in* International conference on machine learning, 448–456.

Kammann, J., A. Malehmir, B. Brodicy, M. Tagliavento, L. Stemmerik, E. Nørmark, H. Lykke-Andersen, and L. Nielsen, 2019, Deep onshore refection seismic imaging of the Chalk Group strata using a 45-kg accelerated weight-drop and combined recording systems with dense receiver spacing: Geophysics, **84**, 259-268.

Kingma, D.P. and J. Ba, 2014, Adam: A method for stochastic optimization: arXiv, 1412.6980.

Janson, X. and D.D. Madriz, 2012, Geomodelling of carbonate mounds using two-point and multipoint statistics: Geological Society, London, Special Publications, **370**, 229-246.

Li, S., C. Yang, H. Sun, and H. Zhang, 2019, Seismic fault detection using an encoder–decoder convolutional neural network with a small training set: Journal of Geophysics and Engineering, **16**, 175-189.

Merrifield, T.P., D.P. Griffith, S.A. Zamanian, S. Gesbert, S. Sen, J. De La Torre Guzman, R.D. Potter, and H. Kuehl, 2022, Synthetic Seismic Data for Training Deep Learning Networks: Interpretation, **10**, 1-52.

Nair, V., and G.E. Hinton, 2010, Rectified linear units improve restricted Boltzmann machines, *in* Proceedings of the 27th international conference on machine learning (ICML-10), 807–814.

Nielsen, L., L.O. Boldreel, T.M. Hansen, H. Lykke-Andersen, L. Stemmerik, F. Surlyk, and H. Thybo, 2011, Integrated seismic analysis of the Chalk Group in eastern Denmark—implications for estimates of maximum palaeo-burial in southwest Scandinavia: Tectonophysics, **511**, 14-26.

Phan, S.D.T., 2021, Machine learning algorithms for solving some seismic inversion challenges: Doctoral dissertation, The University of Texas at Austin.

Qu, D., K. Anderskouv, L. Stemmerik, and L. Nielsen, 2022, Seismic interpretation pitfalls caused by interference effects, exemplified by seismic modeling of outcropping chalk successions: Interpretation, accepted.

Rahman, M.A., and Y. Wang, 2016, Optimizing intersection-over-union in deep neural networks for image segmentation, *in* International symposium on visual computing: Springer, Cham, 234-244.

Ronneberger, O., P. Fischer, and T. Brox, 2015, U-net: Convolutional networks for biomedical image segmentation, *in* International Conference on Medical image computing and computer-assisted intervention: Springer, Cham, 234-241.

Surlyk, F., T. Damholt, and M. Bjerager, 2006, Stevns Klint, Denmark: uppermost Maastrichtian chalk, Cretaceous-Tertiary boundary, and lower Danian bryozoan mound complex: Bulletin of the Geological Society of Denmark, **54**, 1-48.

Surlyk, F., S. L. Rasmussen, M. Boussaha, P. Schiøler, N. H. Schovsbo, E. Sheldon, L. Stemmerik, and N. Thibault, 2013, Upper CampanianeMaastrichtian holostratigraphy of the eastern Danish Basin: Cretaceous Research, **46**, 232-256.

Tarantola, A., 2005, Inverse problem theory and methods for model parameter estimation: Society for Industrial and Applied Mathematics.

van Beers, F., A. Lindström, E. Okafor, and M.A. Wiering, 2019, Deep Neural Networks with Intersection over Union Loss for Binary Image Segmentation, *in* ICPRAM, 438-445.

Wang, Z., T. Chen, X. Hu, L. Wang, and Y. Yin, 2022, A Multi-Point Geostatistical Seismic Inversion Method Based on Local Probability Updating of Lithofacies. Energies, **15**, 299.

Wu, X., L. Liang, Y. Shi, and S. Fomel, 2019, FaultSeg3D: Using synthetic data sets to train an end-to-end convolutional neural network for 3D seismic fault segmentation: Geophysics, **84**, 35-45.

Yuan, H., M. C. Looms, and L. Nielsen, 2021, Rock physics characterization of chalk by combining acoustic and electromagnetic properties: Geophysics, 87, 1-65.

LIST OF FIGURES

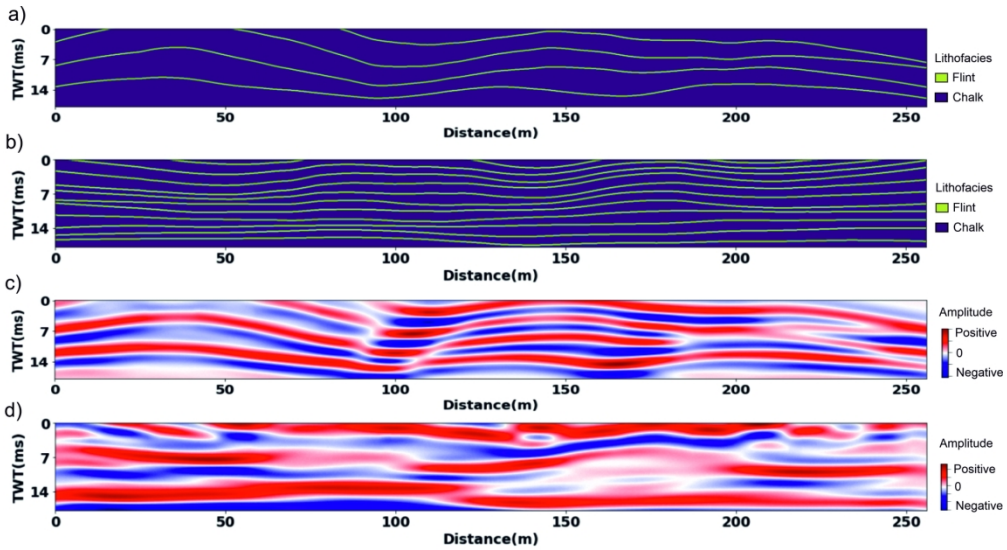

Figure 1. Example synthetic data. (a, b) Two geological sections with different number of layers and varying layer geometry; flint layers in yellow and chalk layers in dark blue; (c, d) Corresponding seismic images.

176x96mm (300 x 300 DPI)

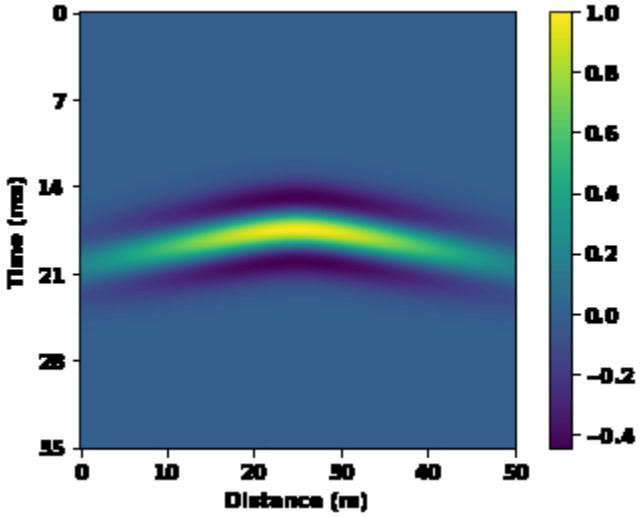

Figure 2. 2D Ricker wavelet matrix with size of 501 × 501; sampling interval is 0.07 ms in time and 0.1 m in space. The 2D wavelet with the 'hyperbolic' shape and the decreasing amplitude away from the center simulates an imperfectly migrated (in this case under-migrated) response from a point scatterer, which is common in real seismic data.

296x241mm (28 x 28 DPI)

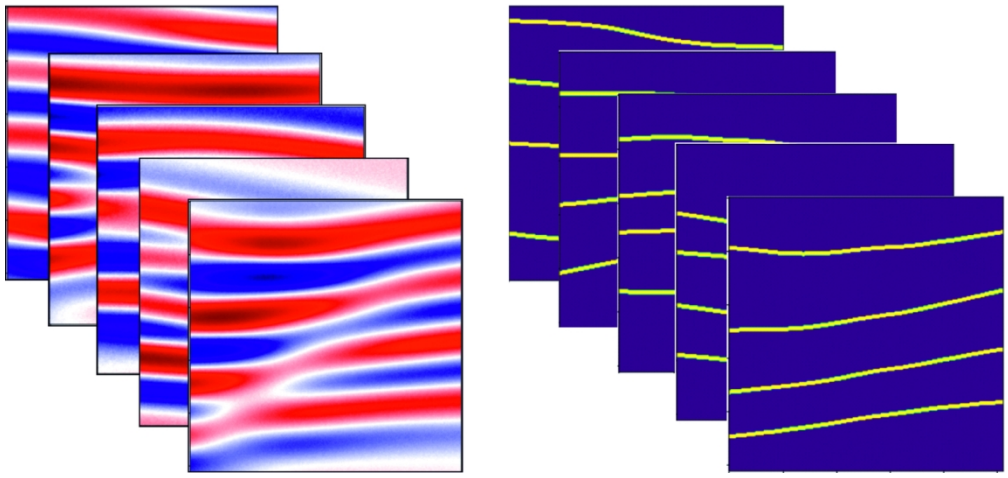

Figure 3. Illustration of patches of seismic images (left) and ground truth geological images (right) used as training data

131x61mm (300 x 300 DPI)

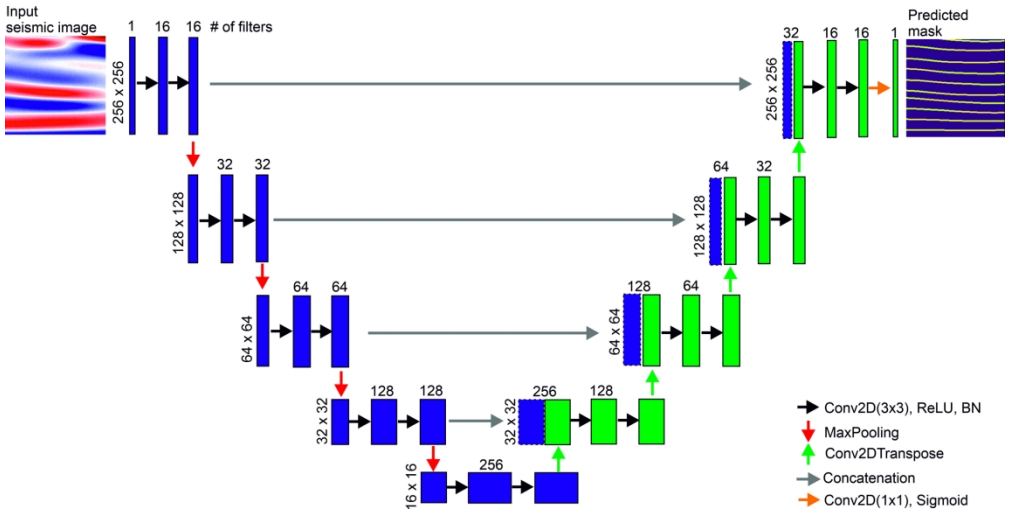

Figure 4. U-net architecture used in this paper

196x98mm (300 x 300 DPI)

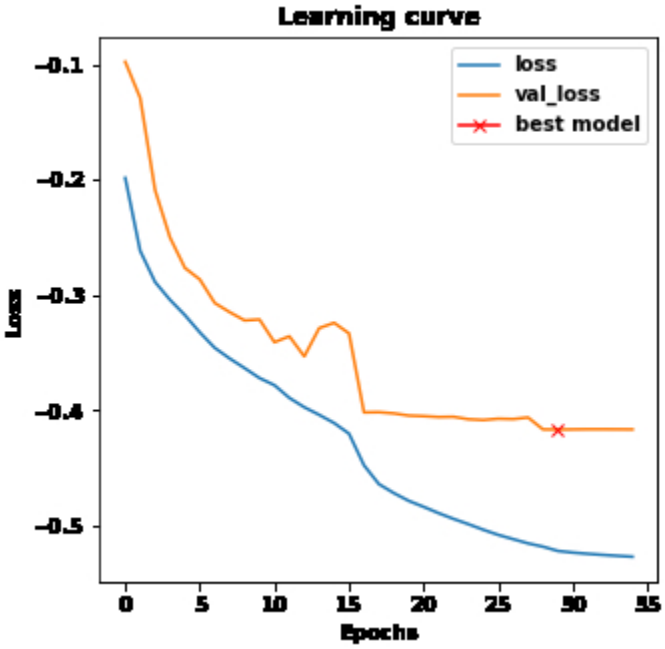

Figure 5. Training and validation loss

310x302mm (28 x 28 DPI)

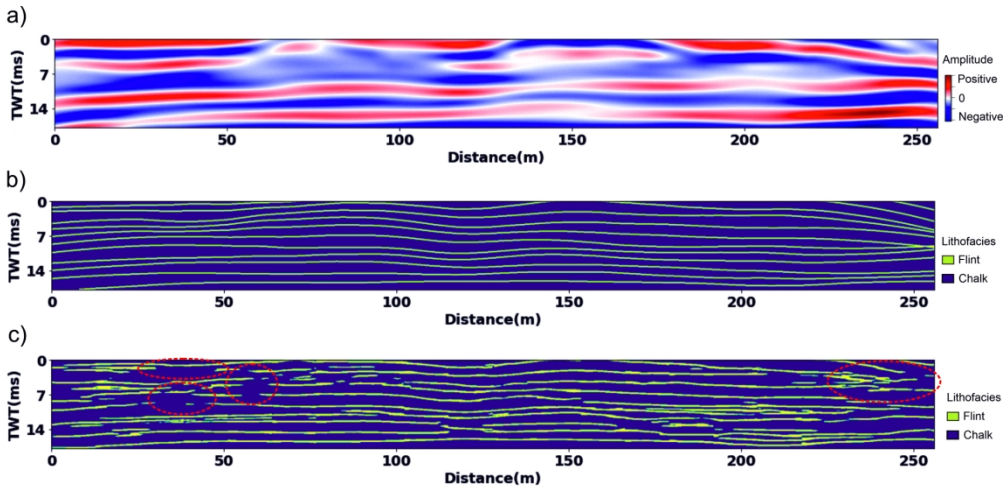

Figure 6. (a) Seismic image with normalized amplitude between -1 and 1; (b) Ground truth label; (c) Predicted flint and chalk layers; the red circles highlight some of the continuity artefacts.

186x90mm (300 x 300 DPI)

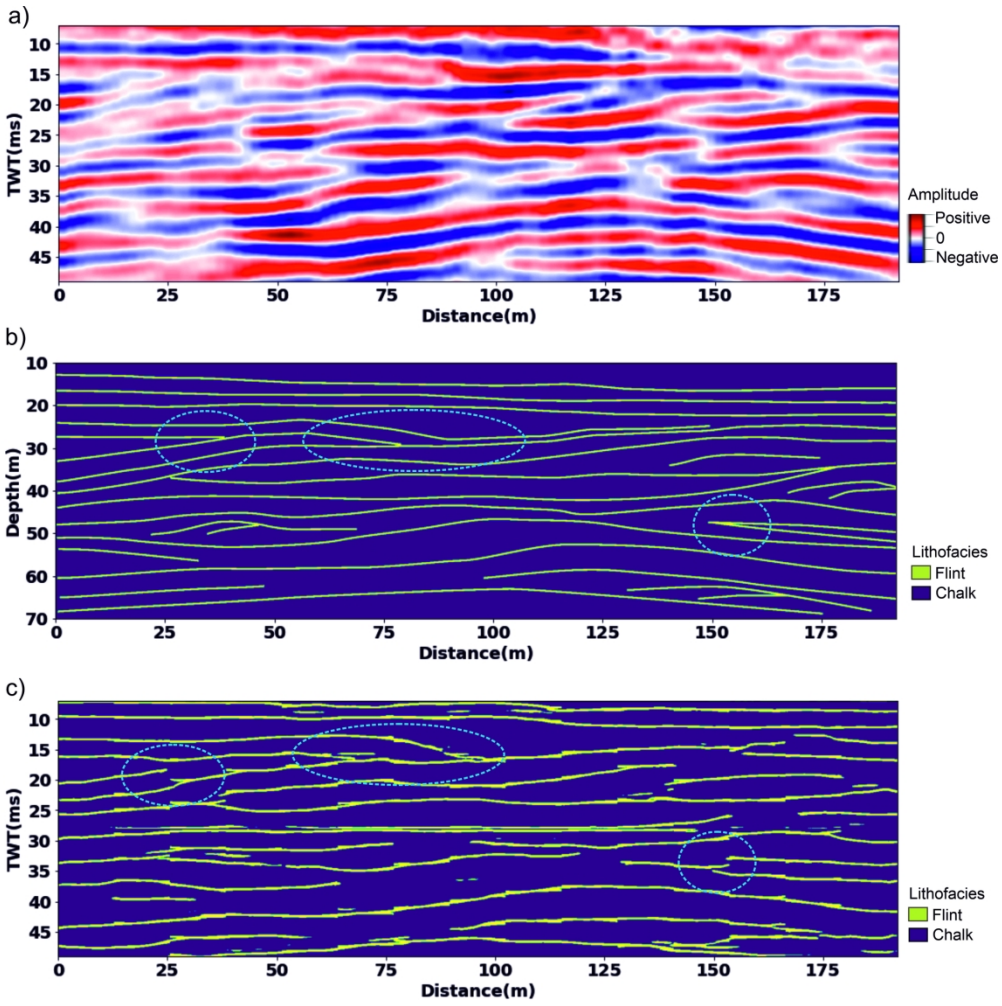

Figure 7. (a) Seismic image with normalized amplitude between -1 and 1, positive in red and negative in blue; (b)Geological section corresponding to the seismic section; the blue circles highlight some complex bedding features not present in the training examples; (c) Predicted flint and chalk layers; the complex bedding features are highlighted with the blue circles.

177x177mm (300 x 300 DPI)

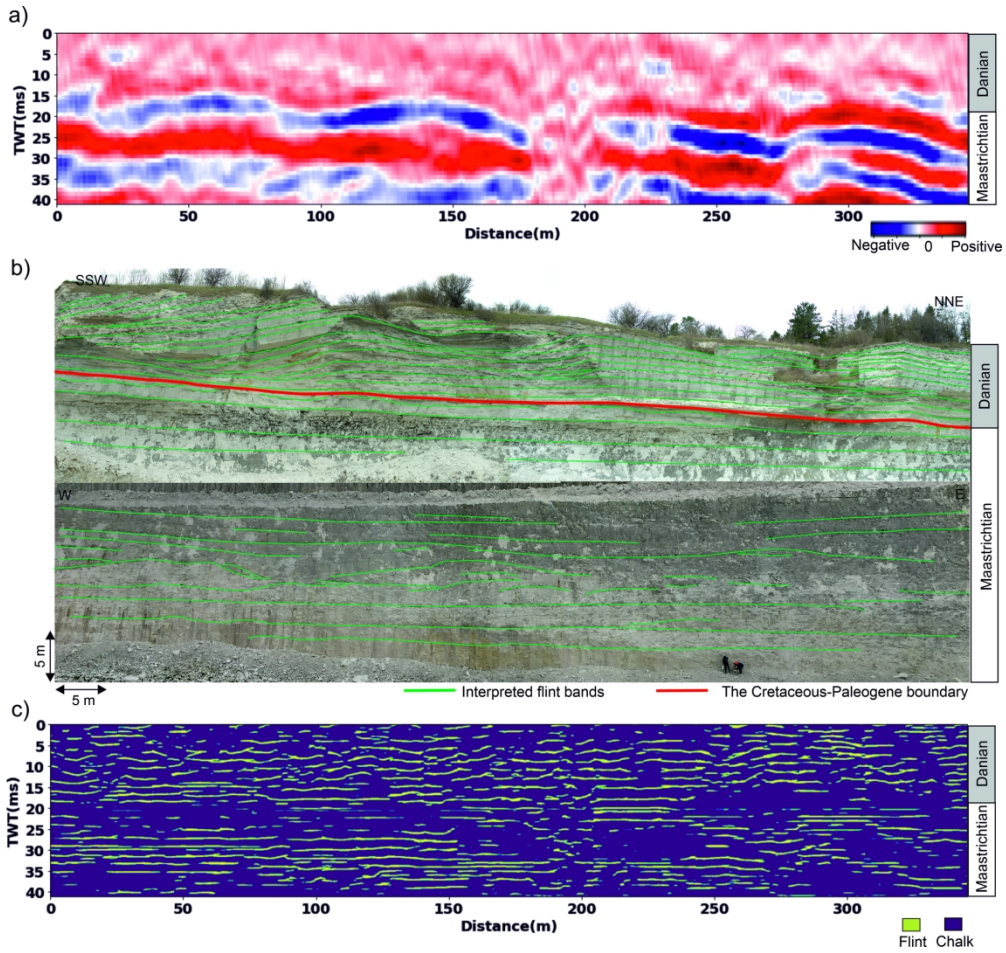

Figure 8. (a) Seismic data collected from the Danian and Upper Maastrichtian chalk succession at the Stevns peninsula in Denmark (Kammann et al., 2019); (b) Stitched image of outcropping chalk succession not far from the seismic profile; the upper section is from the coastal cliffs, the lower section is from a quarry close the cliff; (c) Predicted flint and chalk layers

191x179mm (300 x 300 DPI)